Biochemistry and Biophysics Reports 31 (2022) 101303

Contents lists available at ScienceDirect

Biochemistry and Biophysics Reports

journal homepage: www.elsevier.com/locate/bbrep

# CA10 is associated with HBV-related hepatocarcinogenesis

Kuei-Min Chung [a,b], Ya-Ting Chen [a], Chih-Chen Hong [a,b], Il-Chi Chang [a], Si-Ying Lin [a], Li-Yu Liang [a], Yi-Rong Chen [a], Chau-Ting Yeh [b], Shiu-Feng Huang [a,c,d,*]

[a] Institute of Molecular and Genomic Medicine, National Health Research Institutes, Miaoli, Taiwan
[b] Liver Research Unit, Linko Chang Gung Memorial Hospital, Chang-Gung University, Taoyuan, Taiwan
[c] Department of Anatomic Pathology, Linko Chang Gung Memorial Hospital, Chang-Gung University, Taoyuan, Taiwan
[d] Department of Anatomical Pathology, Chung-Shan Medical University Hospital, Taichung, Taiwan

ARTICLE INFO

*Keywords:*
CA10
HCC
W182 nonsense mutation
miR-27b
HBV

ABSTRACT

Hepatocellular carcinoma (HCC) is the main threat for the patients infected with hepatitis B virus (HBV), but the oncogenic mechanism of HBV-related HCC is still controversial. Previously, we have found that several HBV surface gene (HBS) non-sense mutations are oncogenic. Among these mutations, sW182* was found to have the most potent oncogenicity. In this study, we found that Carbonic Anhydrase X (CA10) level was specifically increased in sW182* mutant-expressing cells. CA10 overexpression was also associated with HBS nonsense mutation in HBV-related HCC tumor tissues. Transformation and tumorigenesis assays revealed that CA10 had significant oncogenic activity. In addition, CA10 overexpression resulted in dysregulation of apoptosis-related proteins, including Mcl-1, Bcl-2, Bcl-xL and Bad. While searching for the regulatory mechanism of CA10, miR-27b was found to downregulate CA10 expression by regulating its mRNA degradation and its expression was decreased in sW182* mutant cells. Moreover, CA10 overexpression was associated with down-regulation of miR-27b in human HBV-related HCC tumor tissues with sW182* mutation. Therefore, induction of the expression of CA10 through repression of miR-27b by sW182* might be one mechanism involved in HBS mutation-related hepatocarcinogenesis.

## 1. Introduction

One of the main complications for chronic hepatitis B virus (HBV) infection is hepatocellular carcinoma (HCC) [1,2], but the mechanism of HBV related carcinogenesis remains controversial [3–5]. It is known that HBV mutations occur frequently to escape from the anti-viral drug therapy or host immune surveillance [6,7]. These HBV mutations may be also related to HCC development. Previously, we have found several HBV surface gene (HBS) non-sense mutations could be oncogenic [8]. These mutations resulted in C-terminal truncation of the HBV surface proteins, which have transcriptional activator function [8,9]. By xenograft experiment, we demonstrated that 3 HBS nonsense mutations (sL95*, sW182*, sL216*) could induce tumor formation in nude mice. The above-mentioned findings all suggest that HBS nonsense mutations are oncogenic and these mutations might play an important role in HBV-related HCC [8]. Among the 3 nonsense mutations, sW182* was found to have the most potent oncogenicity. We have further analyzed the gene expression profiles by microarray study using the stable cell lines harboring wild-type HBS or HBS nonsense mutations and tumors derived from the xenograft experiments. The microarray data was deposited in the GEO database under the accession number GSE50180. Several novel genes which differentially expressed between wild type HBS and nonsense mutants were identified by the expression profiling microarray data, suggesting these genes might be related to HBS mutation-related carcinogenesis. One of those genes is the transforming growth factor beta induced gene (TGFBI). We have reported that dysregulation of the TGFBI gene was involved in the oncogenic activity of the HBV sW182* [10]. We also found that Carbonic Anhydrase X (CA10) is specifically over-expressed in the sW182* mutant cells but not in wild type HBS cells, which suggested that CA10 over-expression might be

*Abbreviations:* HBV, hepatitis B virus; HCC, hepatocellular carcinoma; CA10, Carbonic Anhydrase X; HBS, HBV surface gene; sW182*, HBS gene with W182 nonsense mutation; Mcl-1, myeloid cell leukemia 1 gene; Bcl-2, B-cell lymphoma 2 gene; Bcl-XL, B-cell lymphoma-extra large gene; Bad, BCL2-antagonist of cell death gene.

* Corresponding author. Institute of Molecular and Genomic Medicine, National Health Research Institutes, 35, Keyan Road, Zhunan Town, Miaoli County, 350, Taiwan.
*E-mail address:* sfhuang@nhri.edu.tw (S.-F. Huang).

https://doi.org/10.1016/j.bbrep.2022.101303
Received 25 April 2022; Received in revised form 22 June 2022; Accepted 24 June 2022

involved in the carcinogenesis of sW182*.

CAs are a family of metalloenzymes containing sixteen different isoforms and they have different subcellular localization, tissue distribution and different catalytic activity [11]. They can be subdivided into 5 cytosolic CAs (CA 1, 2, 3, 7 and 13), 5 membrane-associated CAs (CA 4, 9, 12, 14 and 15), 2 mitochondrial CAs (CA 5A and 5B), and one secreted CA (CA 6) [12]. These 13 CAs all have the basic function, i.e. to catalyze the reversible hydration of carbon dioxide to the bicarbonate ion and protons in various physiological and pathological processes. Moreover, CAs also regulate different states of metabolic acidosis, induced by glycolysis and oxidative phosphorylation, and play a relay function in modulating pH regulation and metabolism [13,14]. Many of the CAs have been reported to be overexpressed and implicated in the pathogenesis of human cancers, including liver, lung, breast, colon, renal cell and esophageal squamous cell carcinomas. The cytosolic CA3 overexpression in hepatoma cells could promote the transformation and invasive ability by increasing focal adhesion kinase (FAK) signaling and intracellular and/or extracellular acidification [15]. The membrane-associated CA9 and CA12 overexpression could interfere with the pathways of antitumor activity in the HCC microenvironment [16]. CA9 also has been considered as a good cancer therapeutic target including HCC, since CA9 is involved in pH regulation, cancer stemness and glucose metabolism [17–20]. Thus, CAs have been considered as good drug targets [14,21].

Unlike other mammalian carbonic anhydrases (CAs) family members, CA10 is a secreted and catalytically inactive carbonic-anhydrase homolog which has never been reported to be oncogenic [22]. The study for CA10 is still quite few. Only CA10 mRNA was found to be expressed in kidney, salivary gland, and brain, and shown in low abundance in pancreas, liver, mammary gland, and testis [23]. CA10 might also play an important role in the central nervous system, since CA10 could facilitate surface transport of neurexin and synaptic connections [22]. In this study, we examined the CA10 expressions in human HCC tumor tissues, and performed tumorigenesis assays of CA10. Our results demonstrated that CA10 has oncogenic activity and CA10 overexpression is associated with the carcinogenesis of HBV surface gene (HBS) non-sense mutations. We further demonstrated that sW182* caused decrease of miR-27b level, which then caused the increase of CA10 level. Our results provided a plausible novel oncogenic mechanism for HBV surface gene (HBS) non-sense mutations.

## 2. Materials and methods

### 2.1. Patients and tissues

Two HCC cohorts were obtained for this study. The first cohort was 48 HBV-related HCC tumor tissues and paired benign liver tissue with signed informed consent obtained from the tumor bank of Chang Gung Memorial Hospital (CGMH). DNA and RNA were extracted from the tumor tissues. The second cohort was 46 paired tumor and non-tumor tissue DNA and RNA samples of HBV-related HCC obtained from Taiwan Liver Cancer Network (TLCN), which is now belonged to National Health Research Institutes (NHRI) Biobank. The study protocol has been approved by the Institutional Review Board of CGMH (96-0071B) and National Health Research Institutes, Taiwan (EC0990701 and EC1031102-E). The HBS mutation data of the 48 HBV-related HCC tissues from CGMH already been published in our previous study [8].

### 2.2. Cell culture

Mouse NIH3T3 embryo fibroblast cell line was purchased from Bioresource Collection and Research Center (BCRC Number: 6008), Food Industry Research and Development Institute, Hsinchu, Taiwan. NIH3T3 cells were grown at 37 °C in a humidified 5% $CO_2$ atmosphere with Dulbecco's modified Eagle's medium supplemented with 10% fetal bovine serum (FBS, Gibco), 2 mM of L-glutamine (Gibco) and 1% penicillin/streptomycin (Gibco), and passaged weekly. Human HepG2 hepatoblastoma cell line was purchased from Bioresource Collection and Research Center (BCRC Number: RM60025), Food Industry Research and Development Institute, Hsinchu, Taiwan. HepG2 cells were grown at 37 °C in a humidified 5% $CO_2$ atmosphere with Minimum essential medium supplemented with 10% fetal bovine serum (FBS, Gibco), 2 mM of L-glutamine (Gibco), 0.1 mM non-essential amino acids (Gibco), 1.0 mM sodium pyruvate (Gibco) and 1% penicillin/streptomycin (Gibco), and passaged weekly.

### 2.3. Plasmid constructs and transfection

Human *CA10* gene (NM_020178.4) and *miR-27b* (MI0000440) were cloned into pcDNA6 (Invitrogen, Carlsbad, CA, USA). Human *CA10* short hairpin RNA (shRNA; target sequence: 5′-GGAGCACTTGGTCAACATA-3′) and anti-miR-27b (target sequence: 5′-TTCACAGTGGCTAAGAACTGC-3′) were cloned into pRNA-U6.1/Neo vector (GenScript Corp., Piscataway, NJ, USA). Human CA10 promoter and *CA10* 3′ UTR were cloned into pmirGLO reporter vector (Promega, Madison, WI, USA). The *CA10* 3′UTR containing the mutated *miR-27b* target sequences (CTGTG to GACAC) was constructed by QuickChange II XL Site-Directed Mutagenesis Kit according to the manufacturer's instructions (Stratagene, La Jolla, CA, USA). All constructs were confirmed by direct DNA sequencing. The primer sequences of *CA10*, *miR-27b*, anti-*miR-27b*, *CA10* shRNA, *CA10* promoter and *CA10* 3′UTR are shown in Supplementary Table 1. Transfections were carried out using Lipofectamine 3000 (Invitrogen) according to the manufacturer's instructions and the transfected cells were diluted to select stable clones by blasticidin (Invitrogen) or G418 (Sigma-Aldrich, St. Louis, MO, USA). Established stable cell lines were kept in blasticidin (5 μg/ml) or G418 (5 μg/ml) and then expanded for further studies. All cells were incubated at 37 °C in a humidified 5% $CO_2$ atmosphere, and the media were supplemented with 10% fetal bovine serum (FBS, Gibco), 2 mM of L-glutamine (Gibco), and 1% penicillin/streptomycin (Gibco).

### 2.4. Reverse transcription and quantitative real-time polymerase chain reaction (Q-PCR)

RNAs were extracted from the paired tumor and non-tumor tissues of HCC patients or cultured cells using Trizol reagent (Invitrogen). One microgram of total RNAs was used to synthesize the first strand cDNA using oligo-dT primer and Moloney Murine Leukemia Virus Reverse Transcriptase (Invitrogen). Q-PCR was performed on a Roche LightCycler 480 Real-Time PCR system (Roche Diagnostics). The mRNA levels of each gene were normalized to that of GAPDH and calculated as $2^{-\Delta CT}$ formula (ΔCT = CT of target gene – CT of reference gene; CT is the cycle threshold). All primer sequences are shown in Supplementary Table 1.

### 2.5. Western blot analysis

The primary antibodies used for western blotting were as follows: Bad (Rabbit Bad polyclonal antibody #9292 (1:1000); Cell signaling, Beverly, MA, USA), Bcl-2 (Bcl-2 (D17C4) Rabbit monoclonal antibody #3498 (1:1000); Cell signaling, Beverly, MA, USA), Bcl-xS/L (Bcl-xS/L (S-18) Rabbit polyclonal antibody: sc-634 (1:1000); Santa Cruz, CA, USA), Mcl-1 (Mcl-1 (D35A5) Rabbit monoclonal antibody #5453 (1:1000); Cell signaling, Beverly, MA, USA), CA10 (CA10 Rabbit polyclonal antibody: 12953-1-AP (1:500); Proteintech, Chicago, IL, USA), α-tubulin (α-tubulin Rabbit polyclonal antibody: ab18251 (1:10,000); Abcam, Cambridge, UK), and GAPDH (GAPDH Rabbit polyclonal antibody: GTX100118 (1:20,000); GeneTex, CA, USA). All secondary antibodies were purchased from Jackson Immuno Research (West Grove, PA, USA). For the protein lysate preparation, cells were washed with ice-cold PBS and lysed in RIPA buffer (25 mM Tris-HCl pH 7.6, 150 mM NaCl, 1% NP-40, 1% sodium deoxycholate, 0.1% SDS) containing

indicated protease inhibitors. Protein concentrations were determined by Bradford protein assay and 50 μg of extracted protein were loaded per lane of 10% SDS–PAGE for electrophoresis, and then transferred to polyvinylidene difluoride (PVDF) membrane (Millipore, Bedford, MA, USA). After blocking in TBST buffer (20 mM Tris (pH 7.5), 135 mM NaCl, and 0.1% Tween 20) with 5% milk, the membrane was incubated with a primary antibody (dilution of antibodies was performed according to the manufacturer's instructions) in 5% milk in TBST at 4°C overnight. Following triplicate washes with TBST, the membrane was blotted with a secondary antibody conjugated with horseradish peroxidase (1:10,000 dilution) in TBST with 5% milk for 1 h. The detected proteins were visualized by film exposure using an enhanced chemiluminescence detection system (PerkinElmer, MA, USA).

### 2.6. Cell proliferation assay

Five thousand cells were seeded per well in 96-well culture plates with five replicates and incubated at 37 °C in a humidified incubator for assay with indicated time. MTT solution (0.5 mg/ml, Sigma-Aldrich) was added to each well and then incubated for 4 h at 37 °C. At the end of the incubation periods, the liquid was removed and the remaining formazan pellets in the wells were dissolved with DMSO. The absorbance of the dye was measured at the wavelength of 570 nm with background subtraction at 630 nm by an Ultra Multifunctional Microplate Reader (TECAN).

### 2.7. Clonogenic assay

250 cells per well were plated in six-well plates with duplicate. The cells were then incubated at 37 °C in a humidified incubator for 10 days and colonies were fixed and stained with 0.5% methylene blue (M9140; Sigma-Aldrich, St. Louis, MO, USA) in 50% methanol. Plates were photographed by AlphaImager HP system (ProteinSimple, San Jose, California, USA) and the total number of colonies formed on each well were counted by AlphaEaseFC software.

### 2.8. Soft agar assay

$5x10^3$ cells were suspended in 0.5% low melting agarose as top layer (SeaPlaque; Lonza, Rockland, ME, USA) and plated on the 0.7% solidified bottom layer agarose in six-well plates with duplicate. The plates were incubated at 37 °C in humidified incubator for 21 days and the 0.5 ml complete culture medium of top layer was refreshed every week. For visualization, colonies were stained with 200 μl of 0.1% p-iodonitrotetrazolium violet (I8377; Sigma-Aldrich, St. Louis, MO, USA) at 37 °C in a humidified incubator overnight. Plates were photographed by AlphaImager HP system and the total number of colonies formed on each well were counted by AlphaEaseFC software.

### 2.9. Migration and invasion assay

For migration assay, 0.65 ml of complete culture medium was added into the lower chamber as a chemoattractant and suspended $1 \times 10^4$ cells (0.2 ml) with serum free medium were layered in the upper compartment of the BD Falcon 8.0-μm pore 24-transwell cell culture inserts (BD Biosciences, Franklin lakes, NJ, USA) with duplicate. After incubation for 24 h at 37 °C in a humidified incubator, non-migrating cells were removed from the upper side of the membrane by wiping with a cotton swab. Cells at the lower side of membrane were fixed with 100% cold-methanol and stained with 0.05% crystal violet (Sigma-Aldrich, St. Louis, MO, USA). The pictures of transwell insert membrane were captured at microscope under 12.5× magnification and the total number of migrated cells were counted by AlphaEaseFC software. For invasion assay, the BD Falcon 8.0-μm pore 24-transwell cell culture inserts coated with 100 μl of 0.3 mg/ml Matrigel (BD Biosciences, Bedford, MA, USA) were re-hydrated for 2 h at 37 °C. 0.2 ml of $2 \times 10^4$ cells with serum free medium were layered in the upper compartment of the transwell inserts and then the assays were performed as described in migration assay.

### 2.10. Xenograft studies for tumorigenicity

Male BALB mice were purchased from the National Animal Experimental Center (Taipei, Taiwan). The mice were all maintained in specific pathogen-free conditions. Four-week-old male athymic mice (4–5 for each group) were injected subcutaneously with $1 \times 10^6$ cells in 50 μl of PBS mixed with equal volume of Matrigel. The tumor volume was determined every 3 days by direct measurement with calipers. After 6 weeks, the mice were sacrificed in a $CO_2$ chamber and the tumor tissues were weighted and dissected for cell cultures and histology examination. Portion of tumor tissues were frozen for DNA and RNA extractions. All of the animal studies were done in accordance with the guide for the Care and Use of Laboratory Animals, the National Research Council. The two animal facilities are accredited by Association for Assessment and Accreditation of Laboratory Animal Care International (AAALAC International). The protocol was approved by the NHRI Institutional Animal Care and Use Committee (NHRI-IACUC-105017-A).

### 2.11. Evaluation of endoplasmic reticulum (ER) stress

Evaluation of ER stress marker XBP-1 was performed as previously described [8]. Briefly, RNAs were collected from indicated samples and RT-PCR was performed to determine XBP-1 splicing. Cells treated with brefeldin A (1 μg/ml) (#9972; Cell signaling) for 24 h were used as a positive control.

### 2.12. Luciferase reporter assay

For CA10 promoter reporter assay, HEK293T and Huh7 cells were transfected with 0.1 μg of pGL3-CA10 promoter reporter gene constructs, plus pRL-TK (0.1 μg) and indicated transactivation plasmids (2 μg). For CA10-3′UTR reporter assay, pmirGLO reporter gene constructs and miRNA expression vectors were co-transfected at different ratios in 2 μg per well in HEK293 cells. All cell extracts were prepared 48 h after transfection, and luciferase activities were determined by Dual-Luciferase Reporter Assay System (Promega) following the protocols provided by manufacture. Luciferase activity was assessed by normalization of firefly luciferase activity to Renilla luciferase activity.

### 2.13. Target prediction of miRNAs

Three algorithms, TargetScan, miRanda and PicTar (www.targetscan.org, www.microrna.org, and https://pictar.mdc-berlin.de), were applied to predict candidate miRNAs targeting the 3′-UTR (untranslated region) of *CA10*. Human CA10 was entered in the option of gene ID in these three websites, and miRNAs simultaneously predicted by all three websites were selected for candidate miRNAs.

### 2.14. Nucleotide sequence of the whole HBV genomes

Sequencing analysis of the whole HBV genome in the 46 HBV-related HCC tumor and paired non-tumor tissues from TLCN were performed as described in our previous published report [8].

### 2.15. Analysis of mRNA stability

Cells were treated with 5 μg/ml of actinomycin D (Sigma) for 2–6 h. RNA was extracted using TRIzol reagent (Invitrogen) according to the manufacturer's instructions. Quantitative Real-Time polymerase chain reaction (Q-PCR) was then performed as previously described, with glyceraldehyde-3-phosphate dehydrogenase (GAPDH) used as a normalization control.

### 2.16. Statistical analysis

All statistical analyses were performed using GraphPad Prism software (GraphPad, San Diego, CA, USA). Data are presented as mean ± SD from at least three independent experiments. Group results were compared using Student's *t*-test for continuous variables and Pearson's chi-square test or Fisher's exact test for categorical variables. The differences were significant at a *P* value of less than 0.05.

## 3. Results

### 3.1. CA10 is overexpressed in sW182* mutant cell line and the xenograft tumor

Previously, we have analyzed the gene expression profiles by microarray studies using the NIH3T3 stable cell lines harboring wild-type HBS or HBS nonsense mutations and the tumors derived from the xenograft experiments. The microarray data was deposited in the GEO database under the accession number GSE50180. The microarray data revealed that *Carbonic Anhydrase X* (*CA10*) was the highest expression increase gene in sW182* tumor from the xenograft study when compared with wild-type HBS tumor from the xenograft study. As compared with the NIH3T3 stable cell line harboring wild-type HBS, *CA10* was also found to be highly overexpressed in the NIH3T3 cell line with HBS W182-nonsense mutation by analyzing the expression profiling microarray data. To confirm this result, mRNA and protein expression of CA10 in the sW182* NIH3T3 stable cell line and its xenograft-derived tumor cell line (W182-m1T) were validated by RT-PCR, Q-PCR and western blotting. *CA10* mRNA level was strongly higher in the sW182* stable cell line and its xenograft-derived cell line (W182-m1T) (Fig. 1A & B). Abundant expression of CA10 protein was also detected in the sW182* cell line as compared with vector control or WT (Fig. 1C). Additionally, *CA10* mRNA and protein were also highly expressed in the sW182* HepG2 stable cells (Fig. 1D & E). These results implied that CA10 was up-regulated in sW182* mutant cells.

### 3.2. Tumor tissues of HBV-related HCC patients with HBS W182 non-sense mutation exhibited overexpression of CA10 mRNA

HCC patient samples were examined by Q-PCR for *CA10* expression to examine its correlation with the HBS W182 non-sense mutation (Figs. 1F and S2 Table). Paired tumor and non-tumor liver tissues of 48 HBV-related HCC patients from CGMH were analyzed. The clinical and pathological characteristics of these 48 patients are included in S2 Table. The HBS mutation data of the 48 HBV-related HCC tissues from CGMH has already been published in our previous study [8]. Among these 48 patients, the HCC tumor tissue of 5 patients had sW182* mutation, 37 had wild type HBS, and 6 had other HBS mutation. When the ratio of the *CA10* level of tumor (T) to that of the paired non tumor tissue (N) was higher to one (log T/N ratio >0 represents T/N ratio >1), it was considered as *CA10* up-regulation. Upregulation of *CA10* was significantly associated with genders (p = 0.044), tumor sizes (p = 0.027), and

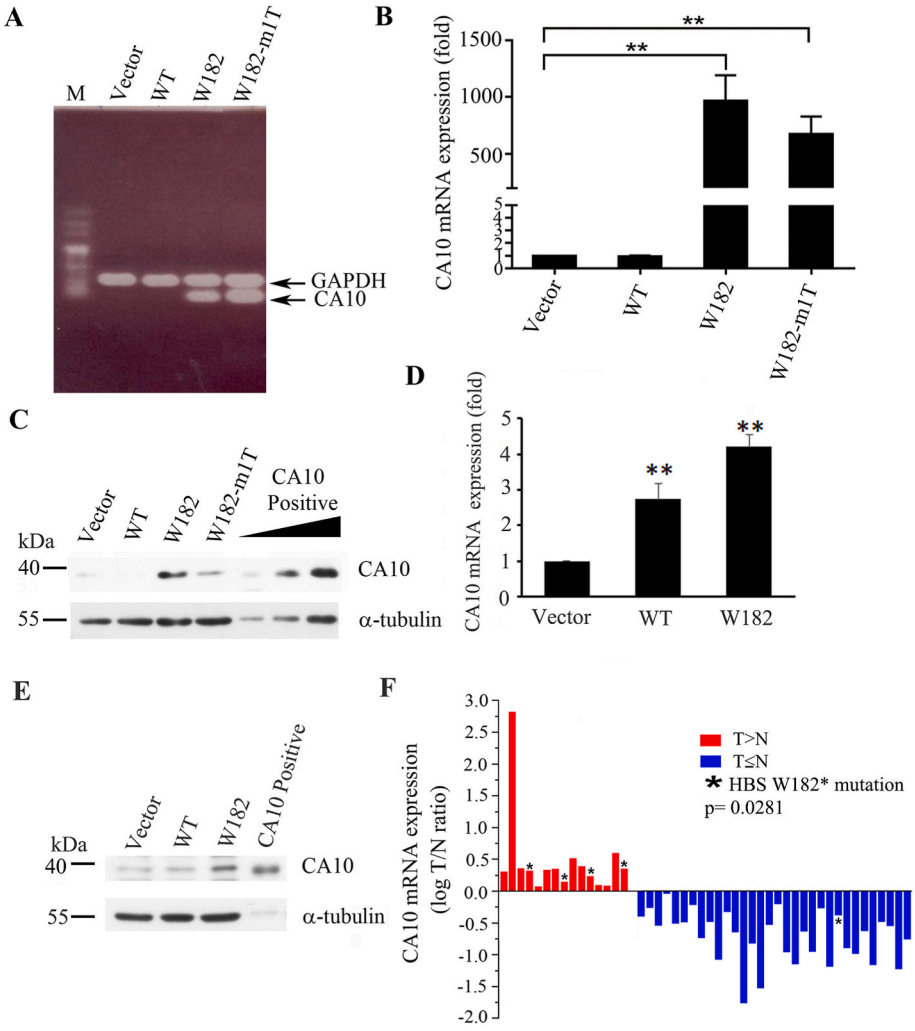


**Fig. 1.** CA10 overexpression is associated with sW182* non-sense mutation. CA10 expressions in sW182* NIH3T3 stable cells and its xenograft-derived cell line (W182-m1T) were compared with vector control or wild type by RT-PCR (A), Q-PCR (B) and western blotting (C), respectively. The CA10 expression in sW182* HepG2 stable cells was also compared with vector control or wild type by Q-PCR (D) and western blotting (E), respectively. (F) *CA10* expressions in the 48 HBV-related HCC tumor (T) and non-tumor tissues (N) from CGMH were analyzed by Q-PCR. Asterisks (*) indicate the tumor had HBS W182 non-sense mutation. Data are represented as mean ± SD from three independent experiments. Statistical significance was determined by Student's unpaired *t*-test. **, P < 0.01.

HBS W182* mutation (p = 0.0281) (Figs. 1F and S2 Table). The result indicates a high correlation between *CA10* overexpression and sW182* mutation.

To further examine its correlation with sW182* mutation, we analyzed the *CA10* expression in the second HCC cohort with 46 HBV-related HCC tumors obtained from TLCN. There were 20 patients had wild type HBS, and 26 had HBS non-sense mutation in their tumor tissues. In the latter 26 patients, 13 had sW182* with or without other non-sense HBS mutations, and the other 13 patients only had non-sense mutation other than sW182* mutations. Q-PCR for *CA10* expression were performed to examine its correlation with sW182* mutation status. When the ratio of the *CA10* expression level of tumor (T) to that of the paired non tumor tissue (N) was higher to one (T/N > 1), it was considered as *CA10* up-regulation. Only 43 of the 46 HBV-related HCC tumors had measurable *CA10* expression. Three patients couldn't detect CA10 expression, one had WT HBS, another one had sW182* mutation and the other one had non-sense mutation other than sW182* mutations. Up-regulation of CA10 expressions were found in 7 of the 12 tumors with sW182* mutation (58.3%), while only 4 of the 19 tumors with wild type HBS had *CA10* up-regulation (21.0%), but the difference was only marginally significant (p = 0.056) (Table 1). In addition, the *CA10* expressions were significantly up-regulated in tumors having sW182* mutations (7/12, 58.3%) when compared with tumors having non-sense mutation other than sW182* mutation (1/12, 8%) (p = 0.027) (Table 1). The results again indicate a high correlation between *CA10* overexpression and sW182* mutation.

The mRNA expression level of *CA10* in 43 HBV-related HCC tumor (T) and non-tumor tissues (N) obtained from TLCN were analyzed by Q-PCR. In these 43 patients, 19 patients had wild type HBS, 12 had sW182*and 12 had other HBS non-sense mutation. WT: patients with wild type HBS gene; W182*: patients with pure or mixed sW182* mutation; Non-W182*: patients with other HBS non-sense mutation. **p value* < 0.05.

### 3.3. *CA10* induced cell proliferation, colony formation, and anchorage-independent growth

CA10 is specifically up-regulated in sW182* mutant cells which indicates CA10 may be associated with the development of sW182* induced HCC. To investigate whether CA10 could promote tumorigenesis, the NIH3T3 stable cells expressing human *CA10* gene were constructed for the transformation and tumorigenesis assays. CA10 protein expression in the stable cells were examined by western blotting (Fig. 2A). To study the oncogenic potential of CA10, proliferation, colony formation and soft agar assays were performed. CA10 apparently induced the cell growth as compared with vector control (Fig. 2B). Colony formation assay showed the colony numbers of CA10 stable cells were obviously increased than that of vector control (Fig. 2C and D). Soft agar assay also showed significant difference between CA10 stable cells and vector control (Fig. 2E and F). The results indicate CA10 promotes cell proliferation and anchorage-independent growth, and thus CA10 may play a role in the malignant transformation in cancer cells.

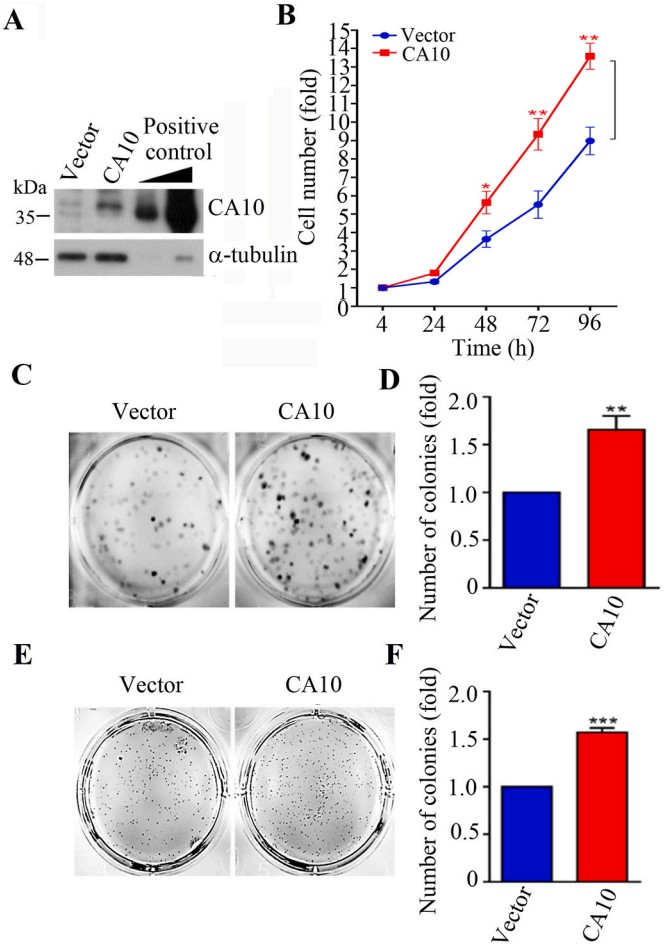


**Fig. 2.** Transforming activity study of CA10 overexpressing NIH3T3 cells. (A) CA10 overexpression in the stable cells were examined by western blotting. (B) Cell proliferation assays for vector control and CA10 overexpressing cells. (C, D) Clonogenic assays of CA10 overexpressing and vector control cells are shown in C and the statistical analysis is shown in D. The total number of colonies formed on each well were counted by AlphaEaseFC software. (E, F) Soft agar assays and the statistical analysis of CA10 overexpressing and vector control cells. Quantifications of cell numbers or colony numbers for CA10 overexpressing cells are presented as fold change in comparison with vector control. Data are represented as mean ± SD from three independent experiments. Statistical significance was determined by Student's unpaired *t*-test. *, $P < 0.05$; **, $P < 0.01$; ***, $P < 0.001$.

**Table 1**
*CA10* Expression in the 43 HBV-related HCC tumors.

Table 1A: The CA10 expressions between wild type HBS and sW182* HCC

| *CA10* expression | WT | W182* | *p value* |
|---|---|---|---|
| *CA10* ↑ | 4 | 7 | 0.056 |
| *CA10* ↓ | 15 | 5 | |
| | 19 | 12 | |

Table 1B: The CA10 expressions between sW182* and other non-sense HBS mutation HCC

| *CA10* expression | W182* | Non-W182* | *p value* |
|---|---|---|---|
| *CA10* ↑ | 7 | 1 | 0.027* |
| *CA10* ↓ | 5 | 11 | |
| | 12 | 12 | |

### 3.4. *Cell migration and invasion are increased in the CA10 overexpressing cells*

Furthermore, we aimed to determine whether CA10 might play a vital role in the cell migration. The transwell migration assays were performed in the presence of 10% FBS to measure spontaneous migration. For cell migration assay, the numbers of migrated cells for CA10 stable cells were significantly increased than that of vector control (Fig. 3A and B). In transwell invasion assay, CA10 stable cells also showed enhanced invasion as compared to vector control (Fig. 3C and D). The results suggest that CA10 might promote higher mobility and/or enzymatic activity for degrading ECM components to achieve invasion.

### 3.5. *CA10 significantly promoted tumorigenesis in the xenograft study*

All results of tumorigenesis assays suggest that CA10 has significant

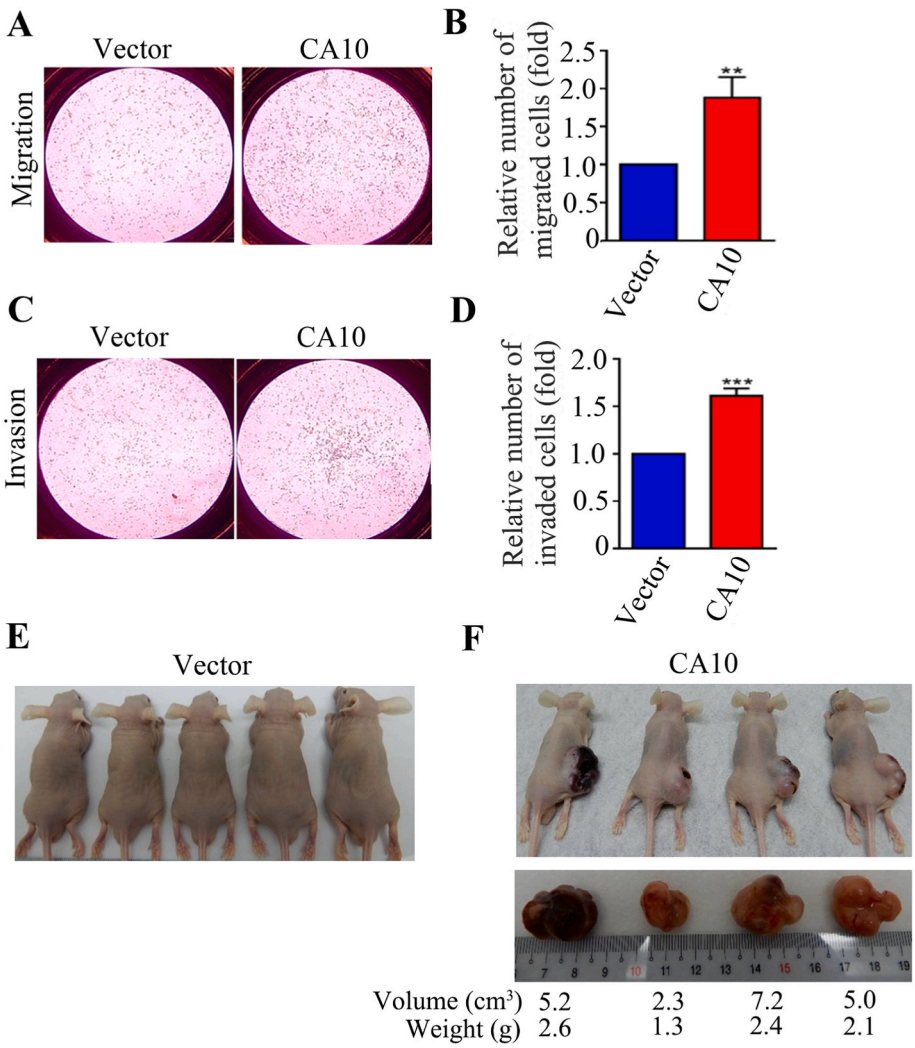


**Fig. 3.** Migration/invasion and xenograft study of CA10 overexpressing cells. (A, B) Transwell migration assays of CA10 overexpressing cells or vector control. Photographs of 24-transwell insert membrane in a representative experiment are shown in A and the statistical analysis is shown in B. (C, **D**) Transwell invasion assays of CA10 overexpressing cells or vector control. Representative images are shown in C and the statistical analysis is shown in D. Quantification of migrated/invaded cell numbers for CA10 stable cells presented as fold change in comparison with vector control. Data are represented as mean ± SD from three independent experiments. Statistical significance was determined by Student's unpaired *t*-test. *, $P < 0.05$; **, $P < 0.01$; ***, $P < 0.001$. (E) Xenograft study of vector control. (F) Xenograft study of CA10 stable cells showed tumor formation in all four mice. Tumor volume was measured with a caliper and calculated by using the formula $a \times b^2 \times 0.5$, where a and b represented the larger and smaller diameters, respectively.

oncogenic activity. To confirm the role of CA10 in tumor progression, we established the mouse xenograft model. Male athymic BALB/c nude mice of 4-week-old received subcutaneous injection of the stable cells overexpressing CA10 or vector. None of the five nude mice injected with vector control cells had tumor growth at the end of 6 weeks (Fig. 3E), while all four nude mice injected with CA10 stable cells had large tumor formation (Fig. 3F). The results indicated that CA10 significantly promoted *in vivo* tumor progression.

### 3.6. CA10 has anti-apoptotic effect but not an ER stress inducer

To understand whether apoptosis or ER stress played a role in the CA10-induced tumorigenesis, the apoptosis-related protein expression profiles and the ER stress markers were examined by western blot analysis and RT-PCR, respectively. When comparing CA10 stable cells with vector control, CA10 had an obvious increase of anti-apoptotic protein myeloid cell leukemia 1 (Mcl-1), B-cell lymphoma 2 (Bcl-2) and B-cell lymphoma-extralarge (Bcl-xL), and decrease of the apoptotic protein BCL2-antagonist of cell death (Bad) (Fig. 4A). To further confirm the data, we knock-downed CA10 by CA10 shRNAs in CA10 stable cells and got a complete opposite result. Down-regulation of CA10 certainly decreased the expression of anti-apoptotic protein Mcl-1, Bcl-2 and Bcl-xL and increased the expression of the apoptotic protein Bad (Fig. 4B).

To understand if CA10 could cause ER stress, the activation of ER stress-induced UPR targets in CA10 overexpressing cells were examined by western blotting. Cells treated with Brefeldin A (BFA) were used as the positive control of ER stress. CA10 didn't induce the phosphorylation of IRE1α and the expression level of IRE1α (Fig. 4C). As compared with vector control, no induction of ATF6 cleavage or ATF4 expression was detected in the CA10 overexpressing cells (Fig. 4D and E). Consistently, there was no change in the status of ER stress marker XBP-1 in CA10 overexpression (Fig. 4F). These results suggested that CA10 could inhibit apoptosis but couldn't induce ER stress.

### 3.7. CA10 is the target gene of miR-27b

To examine the transcriptional regulatory mechanism of CA10 overexpression in sW182* cells, the upstream DNA sequence of CA10 promoter according to Ensembl Genome Browser database (http://www.ensembl.org/index.html) was cloned for luciferase promoter reporter assay. There were no differences in the reporter activity between sW182* and wild type or vector control (Fig. 5A), indicating CA10 transcription was not disturbed by sW182* mutant.

The increase of mRNA amounts at steady state may result from post-transcriptional regulation. Therefore, different on-line algorithms (TargetScan, miRanda and PicTar) were used to filter out candidate miRNAs predicted for targeting *CA10* 3′UTR. Four candidate miRNAs (miR-27a, miR-27b, miR-128 and miR-185) simultaneously predicted by all three websites were selected (Fig. 5B). Expression levels of the 4 miRNAs in sW182* NIH3T3 stable cells were examined by Q-PCR. As compared with vector control, there was no change in the expression level of miR-27a, miR-128 or miR-185 in sW182* NIH3T3 stable cells

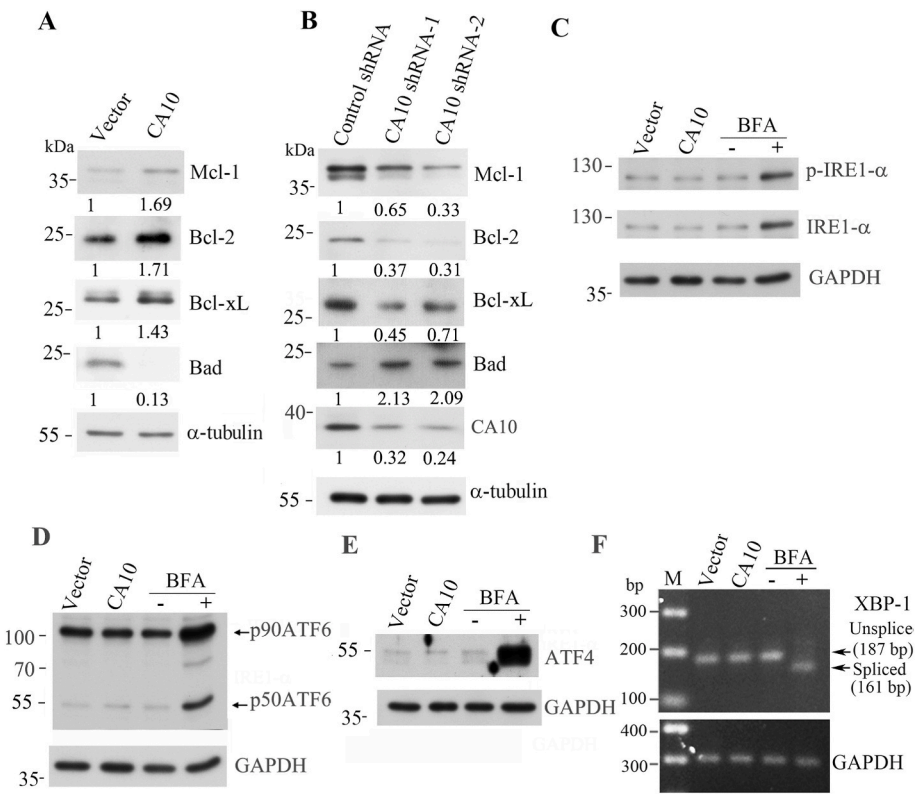


**Fig. 4.** Apoptosis-related protein expression profiles and the ER stress markers of CA10 overexpressing cells were examined by western blot analysis and RT-PCR, respectively. Apoptosis related signaling protein levels were measured by western blotting in the CA10 overexpressing stable cells (A) or CA10 knock-down stable clones: shCA10-1 and shCA10-2 (B). Band intensity given underneath gel image was determined with ImageJ software, presented as fold change compared with controls, respectively. (C) Phosphorylation of IRE1α was examined by western blotting. (D) ATF6 cleavage was evaluated by western blotting. (E) ATF4 expression was determined by western blotting. (F) Splicing of XBP-1 mRNA was examined by RT-PCR. The un-spliced and spliced forms of XBP-1 were indicated by arrows. GAPDH was used as a loading control.

(Supplementary Fig. 1). Only miR-27b was markedly down-regulated in the sW182* expressing cells and its xenograft-derived cells when compared to that of wild type HBS or vector control (Fig. 5C). Meanwhile, we observed a potential binding site for miR-27b in the 3′-UTR of *CA10* (Fig. 5D). As shown in Figs. 5D and 3′-UTR of *CA10* contained complementary regions of miR-27b. Luciferase reporter assays showed that miR-27b significantly inhibited the luciferase activity of wild type *CA10*-3′UTR in a dose-dependent manner (Fig. 5E, left panel). Moreover, the miR-27b binding site was conserved at *CA10* 3′UTR among vertebrates (Fig. 5D). To further confirm the direct interaction of miR-27b with *CA10* 3′UTR, we constructed a mutant CA10 3′UTR consisting of mutations at the seed region of miR-27b binding site for the luciferase reporter assay. The mutant sequences of *CA10* 3′UTR are shown in Fig. 5D. The reporter assay demonstrated that miR-27b lost the suppressive luciferase activity on mutant *CA10*-3′UTR (Fig. 5E, right panel), indicating miR-27b dominantly bound to the seed sequences within the *CA10*-3′UTR and leaded to degradation of the mRNA. These data indicated that miR-27b targeted the 3′-untranslated region (3′-UTR) of *CA10*.

### 3.8. *sW182* may post-transcriptionally regulate CA10 expression via decreasing miR-27b expression*

To understand whether the induction of *CA10* expression by sW182* was through repression of miR-27b, miR-27b expressions in sW182* HepG2 stable cells were examined by Q-PCR. We found that miR-27b was markedly down-regulated in sW182* HepG2 stable cells (Fig. 6A). To confirm that miR-27b could negatively regulate *CA10* mRNA expression in sW182* cells, miR-27b expression plasmid was transfected into sW182* HepG2 stable cell line and then the *CA10* mRNA expression was detected by Q-PCR. After transfection with miR-27b plasmid, the miR-27b expression level in sW182* HepG2 stable cells was increased to 1.3-fold as compared with vector control (Fig. 6B). The increased expression of miR-27b was accompanied by the decreased expression of *CA10* mRNA (Fig. 6C, $P = 0.005$). Immunoblotting data indicated that miR-27b overexpression reduced the expression of CA10 protein in sW182* HepG2 stable cells (Fig. 6D). To confirm the result, we tested the *CA10* mRNA expression level after transfection with the anti-miR27b expression plasmid. The expression level of miR-27b in sW182* HepG2 stable cells after transfection with the anti-miR-27b plasmid was decreased to 0.6-fold as compared with vector control (Fig. 6B). The decreased expression of miR-27b was coincided with increased expression of *CA10* mRNA in sW182* stable cells (Fig. 6C, $P = 0.007$). Immunoblotting data also revealed that decreased expression of miR-27b increased the expression of CA10 protein in sW182* HepG2 stable cells (Fig. 6D). All of these results showed that miR-27b down-regulated *CA10* expression and CA10 overexpression in sW182* cells may be due to decreased expression of miR-27b. For better understanding that CA10 mRNA is the target of miR-27b, the effect of miR-27b on CA10 mRNA stability was analyzed in sW182* stable cells. When sW182* HepG2 stable cells were transfected with the miR-27b expression plasmid, an increase in mRNA degradation occurred as compared to vector control (Fig. 6E). The data reveled that miR-27b inhibited CA10 expression by regulating its mRNA degradation. Further, our results suggest that sW182* down-regulated miR-27b, which in turn caused the increase of CA10.

### 3.9. *CA10 overexpression is associated with down-regulation of miR-27b in HBV-related HCC tumors with sW182* mutation*

For miR-27b expression, we had analyzed the miR-27b expression in the second HCC cohort with 46 HBV-related HCC tumor (T) and non-tumor tissues (N) obtained from TLCN. Thirty-four of the 46 HBV-related HCC tumors (34/46, 73.91%) had down-regulation of miR-27b, and there was no significant difference between wild type and non-sense mutation of HBS ($p = 1.0$). Among the 34 HCC tumors with miR-27b down-regulation, 32 had measurable CA10 expression. The 2 patients with undetectable CA10 expression include one had sW182* mutation and the other one had non-sense mutation other than sW182* mutations. Among the 32 HBV-related HCC tumors with miR-27b down-

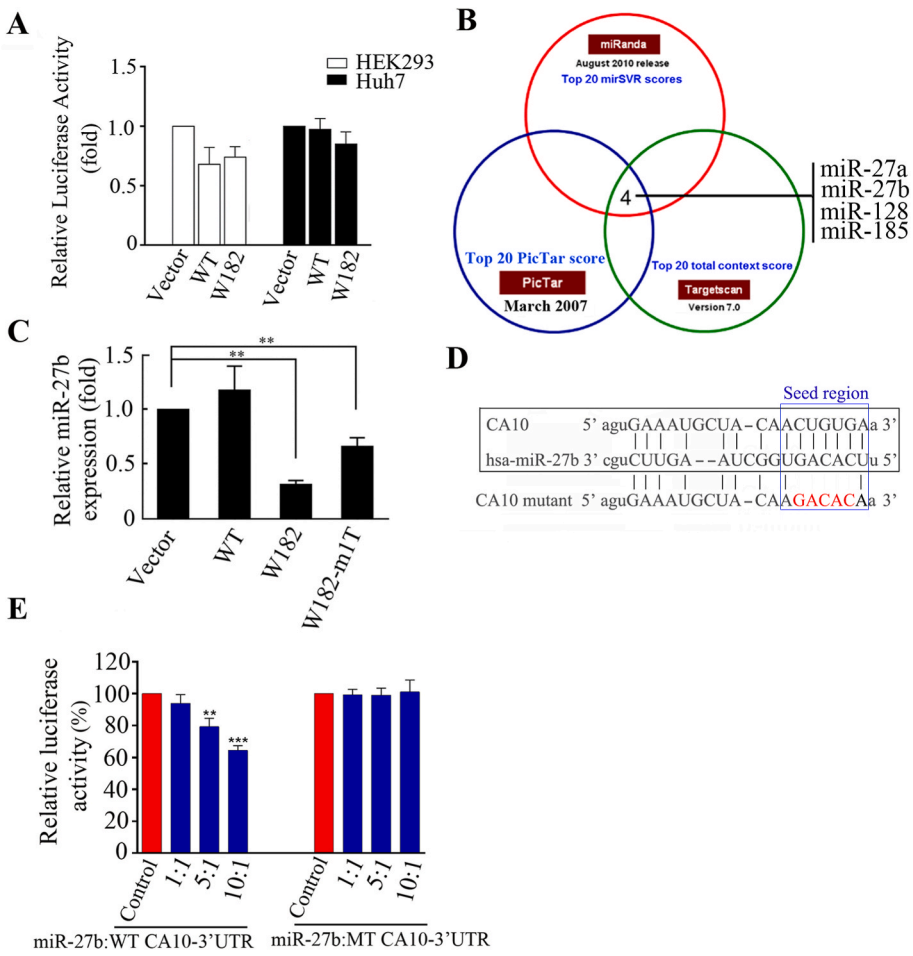


**Fig. 5.** miR-27b targeted the 3′-untranslated region (3′-UTR) of *CA10*. (A) The *CA10* promoter reporter plasmid was co-transfected with plasmids expressing wild type (WT) HBS or sW182* in HEK293 cells and Huh7 cells. Dual-Luciferase Reporter Assay system was performed for the promotor reporter assay. **(B)** miRNAs potentially targeting *CA10* were predicted by the TargetScan, miRanda and PicTar. Venn diagram showed that there were only 4 candidate miRNAs (miR-27a, miR-27b, miR-128 and miR-185) selected by all 3 databases. **(C)** Q-PCR analysis of miR-27b expression in WT or sW182* NIH3T3 stable cells and its xenograft-derived cells (W182-m1T). (D) The miR-27b target region of human *CA10* 3′UTR. The mutant *CA10* 3′UTR consisting of mutations at the miR-27b binding site and red words indicate the mutated sequences. **(E)** Dual-Luciferase Reporter Assay of wild-type and mutant *CA10*-3′UTR while co-transfected with miR-27b at different ratios. Control treatment was cells only transfected with wild-type or mutant *CA10*-3′UTR reporter plasmid. Data was represented as mean ± SD from three independent experiments. Statistical significance were determined by Student's unpaired *t*-test. **, $P < 0.01$; ***, $P < 0.001$. (For interpretation of the references to color in this figure legend, the reader is referred to the Web version of this article.)

regulation, 4 of the 15 tumors with wild type HBS (26.7%), and 1 of the 9 tumors with other non-sense mutations of HBS (11.1%), had up-regulation of *CA10* (Table 2). While 4 of the 8 tumors with sW182* mutation had up-regulation of CA10 (50%) (Table 2). The difference of CA10 overexpression between wild type and sW182* were not significant due to small case number. The above results demonstrated that *CA10* up-regulation could be associated with down-regulation of miR-27b in HCC, especially in HCC with sW182* mutation. However, the association is not very strong, suggesting the involvement of additional factors.

The mRNA expression level of *CA10* in 32 miR27b down-regulated patients carrying WT HBS, sW182* and other HBS non-sense mutation were analyzed by Q-PCR. In these 32 patients, 15 patients had wild type HBS, 8 had sW182*and 9 had other HBS non-sense mutation. WT: patients with wild type HBS gene; W182*: patients with pure or mixed sW182* mutation; Non-W182*: patients with other HBS non-sense mutation.

## 4. Discussion

In this study, we identified CA10 as a novel factor in the HCC pathogenesis. We found that overexpression of CA10 induced cell proliferation, colony formation and promoted cell migration/invasion in NIH3T3 cells. It significantly promoted tumorigenesis in the xenograft study. The above results are similar with previous reports for CA8 and CA11 that promote tumor proliferation and invasion *in vitro* [24–26]. In addition, CA10 overexpression resulted in dysregulation of apoptosis-related proteins, including Mcl-1, Bcl-2, Bcl-xL and Bad. Apoptosis has been reported to play an important role in HCC development [27,28]. Apoptosis related proteins, such as Mcl-1, Bcl-2 and Bcl-xL, all have been reported to be involved in the progression of HCC and are considered as potential targets for anti-HCC therapy [29,30]. Moreover, previous study demonstrates that CA9 is involved in hexokinase II inhibitor-induced hepatocellular carcinoma apoptosis [20]. However, CA10 belongs to CA-RPs which is catalytically inactive [31]. Therefore, the oncogenic potential of CA10 demonstrated in this study might be different from those catalytically active CAs such as CA9 which regulates an acidic extracellular microenvironment for tumor development [32]. In addition, CA-RPs are known to participate in signaling pathway by secretory ligand and protein-protein interaction, which is different from other CAs with catalytic activity [22,33,34]. These reports verified the mechanism of oncogenic activity of CA-RPs is through non-catalytic pathway. CA10 is likely oncogenic through a novel non-catalytic pathway.

We found that both CA10 mRNA and protein levels are elevated by sW182*. However, the reporter assay showed no direct transcriptional regulation in *CA10* promoter by sW182*. Therefore, we have searched for the candidate miRNAs that play a role in post-transcriptional regulation of *CA10*. We found that miR-27b was markedly downregulated in the sW182* cells. Reporter assays demonstrated that miR-27b post-transcriptionally regulated CA10-3′UTR in a dose-dependent manner. Moreover, CA10 up-regulation was associated with down-regulation of miR-27b in HCC with sW182* mutation. The above results support the assumption that down-regulation of miR-27b is associated with HBS nonsense mutation and results in overexpression of CA10, which may play a role in HBV associated hepato-carcinogenesis. There are already multiple reports focused on the role of miRNAs in HBV infection and hepatocellular carcinoma [35,36]. Among them, miR-27b has been

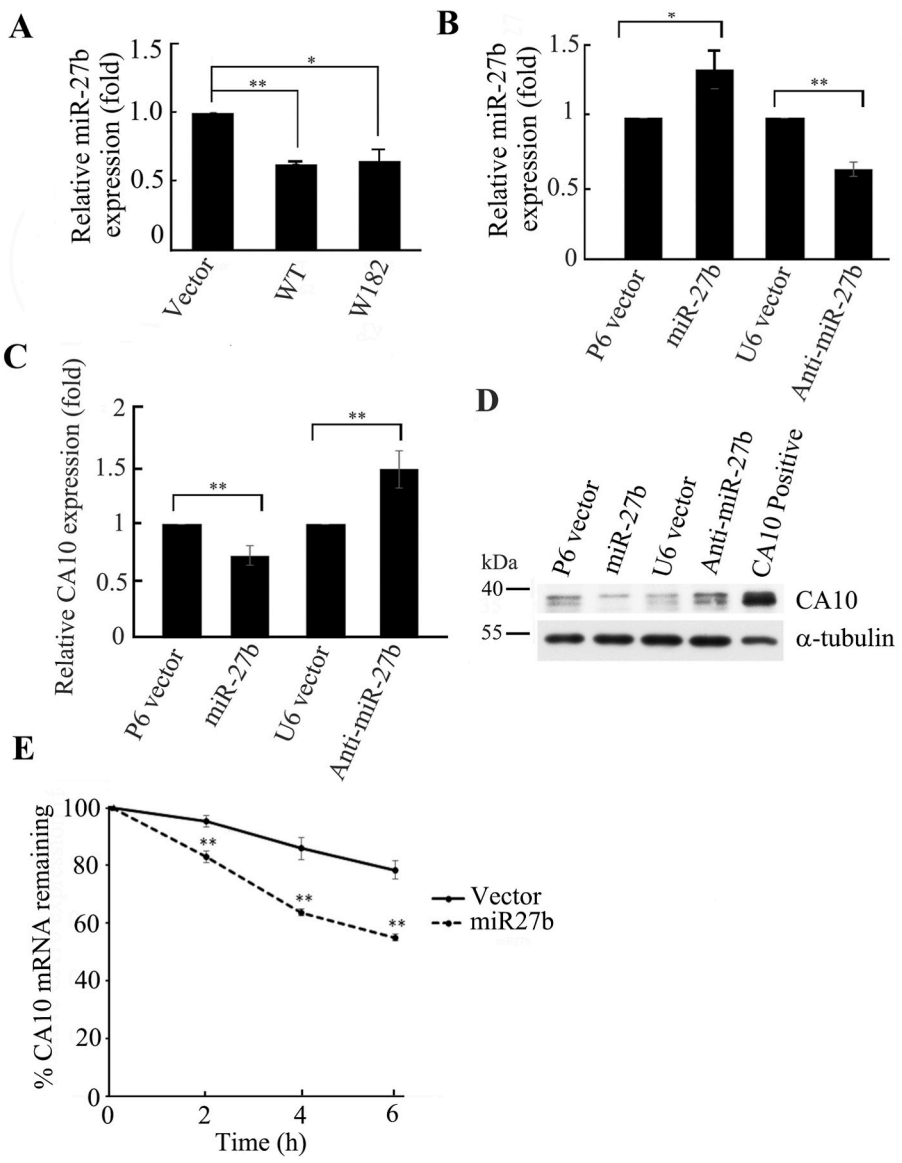


**Fig. 6.** CA10 overexpression in sW182* stable cells might be through repression of miR-27b. (A) Q-PCR analysis of miR-27b expression in WT or sW182* HepG2 stable cells. (B) Q-PCR analysis of miR27b expression in sW182* HepG2 stable cells after transient transfection with vector, miR-27b or anti-miR-27b plasmid. (C) Q-PCR analysis of *CA10* mRNA expression in sW182* HepG2 stable cells after transient transfection with vector, miR-27b or anti-miR-27b plasmid. (D) Western blot analysis of CA10 expression in sW182* HepG2 stable cells after transient transfection with vector, miR-27b or anti-miR-27b plasmid. (E) CA10 mRNA degradation was measured by real-time Q-PCR in sW182* HepG2 stable cells following transient transfection with vector or miR-27b plasmid. Data was represented as mean ± SD from three independent experiments. Statistical significance were determined by Student's unpaired *t*-test. *, $P < 0.05$; **, $P < 0.01$.

**Table 2**
*CA10* expression in the 32 HBV HCC with miR27b down-regulation.

Table 2A: The CA10 expressions between wild type HBS and sW182* HCC

| *CA10* expression | WT | W182* | *p value* |
|---|---|---|---|
| *CA10* ↑ | 4 | 4 | 0.371 |
| *CA10* ↓ | 11 | 4 | |
| | 15 | 8 | |

Table 2B: The CA10 expressions between sW182* and other non-sense HBS mutation HCC

| *CA10* expression | W182* | Non-W182* | *p value* |
|---|---|---|---|
| *CA10* ↑ | 4 | 1 | 0.131 |
| *CA10* ↓ | 4 | 8 | |
| | 8 | 9 | |

found to function as a tumor suppressor and is downregulated in many human cancers including breast, colon, gastric, lung, prostate, and renal cancers [37–39]. In GSE53872 microarray data, miR-27b is down-regulated in liver and kidney cancers. Recently, a study from Hu et al. also shows that the expression of miR-27b in HCC is lower than that in adjacent nontumor tissues [40]. The above results all support that downregulation of miR-27b might be involved in the carcinogenesis of HBS nonsense mutant.

In summary, overexpression of CA10 was associated with significant oncogenic activity and inhibited apoptosis by dysregulation of apoptosis-related proteins, including Mcl-1, Bcl-2, Bcl-xL and Bad. Additionally, CA10 expression was downregulated by miR-27b. Moreover, CA10 overexpression was significantly associated with HBS nonsense mutation in two HCC cohorts. The results on the HCC cohort also revealed that CA10 up-regulation was associated with down-regulation of miR-27b in HCC with sW182* mutation. Our results support a model for the up-regulation of CA10 in sW182* cells. sW182* could repress miR27b expression and result in overexpression of CA10 to promote cell proliferation, cell migration and inhibit apoptosis. Therefore, induction of the overexpression of CA10 may give rise to HBV-related HCC (Fig. 7). The cause of miR-27b down-regulation upon sW182* nonsense mutation remains unclear. MicroRNA-27b is often down-regulated in several types of cancers, and hypermethylation of the promoter area is a major mechanism for dysregulation of miR-27b in gastric cancer and colorectal cancer [41,42]. Promoting DNA methyltransferases (DNMTs) working on the promoter region of target genes is a way to hypermethylation of the promoter area [43,44]. Although HBS or its mutants have never been reported to directly bind to DNA or a

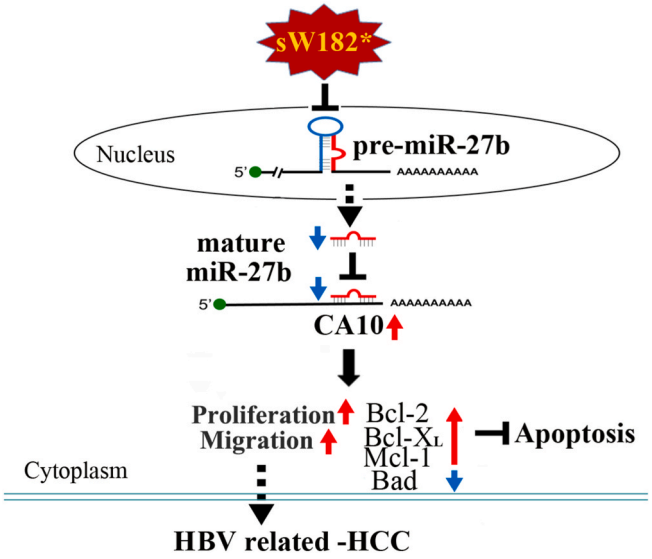


**Fig. 7.** A schematic diagram illustrating induction of the oncogenic activity of CA10 through repression of miR-27b by HBS W182 non-sense mutation. sW182* could repress miR-27b expression and subsequently up-regulate CA10. Finally, CA10 overexpression could result in promotion of cell proliferation, cell migration and reduction of apoptosis by dysregulation of apoptosis-related proteins, suggesting that CA10 may play a role in hepatocarcinogenesis.

DNA methyltransferase, our microarray data showed a much higher expression of DNMT1 in the sW182* mutant cells (data not shown). Additionally, HBS and its C-terminal truncation mutants have transcriptional activator function. We proposed a hypothesis that sW182* down-regulated miR-27b expression possibly by aberrant DNA methylation of the promoter area through activation of the related signal pathway that upregulated the expression of DNA methyltransferases. Further study is necessary for validation the possible mechanism of sW182*-mediated down-regulation of miR-27b. More mechanisms will be further explored on the role of HBS nonsense mutation in hepato-carcinogenesis.

## Declaration of competing interest

The authors declare that they have no known competing financial interests or personal relationships that could have appeared to influence the work reported in this paper.

## Data availability

No data was used for the research described in the article.

## Acknowledgements

This work was supported by grants from National Health Research Institutes for Shiu-Feng Huang [NHRI -A1-MG-093-PP-04, NHRI -A1-MG-096-PP-04, NHRI-A1- MG-103-PP-04, NHRI-A1- MG-105-PP-04], National Science Council for Shiu-Feng Huang [NSC92-2320-B-400–002, NSC97-2320-B-400-006-MY3], and Ministry Of Science and Technology [MOST 105-2320-B-400-014-MY2]. The funders had no role in study design, data collection and analysis, decision to publish, or preparation of the manuscript. The authors thank Dr. Y. Henry Sun in NHRI for his suggestions, review and editing the manuscript.

## Appendix A. Supplementary data

Supplementary data to this article can be found online at https://doi.org/10.1016/j.bbrep.2022.101303.

## References

[1] Hepatitis B. virus, The Major Etiology of Hepatocellular Carcinoma - PubMed [cited 6 Aug 2021]. Available: https://pubmed.ncbi.nlm.nih.gov/2834034/.
[2] D.G. AMP, Hepatitis B virus infection–natural history and clinical consequences, N. Engl. J. Med. 350 (2004) 1118–1129, https://doi.org/10.1056/NEJMRA031087.
[3] Y.W. CN, MAB, Mechanisms of HBV-related hepatocarcinogenesis, J. hepatol. 52 (2010) 594–604, https://doi.org/10.1016/J.JHEP.2009.10.033.
[4] McMahonBJ. LokASF, Chronic hepatitis B, Hepatology 45 (2007) 507–539, https://doi.org/10.1002/HEP.21513.
[5] KelleyRK. LlovetJM, SingalAG. VillanuevaA, RoayaieS. PikarskyE, et al., Hepatocellular carcinoma, Nat. Rev. Dis. Prim. 7 (1) (2021), https://doi.org/10.1038/s41572-020-00240-3, 2021;7: 1–28.
[6] F.Z. SL, Molecular genetics of HBV infection, Antivir. Ther. 15 (Suppl 3) (2010) 3–14, https://doi.org/10.3851/IMP1619.
[7] JMP, The concept of hepatitis B virus mutant escape, J. Clin. Virol. : off. pub. Pan Am. Soc. Clinic. Virol. 34 (2005), https://doi.org/10.1016/S1386-6532(05)80021-6. Suppl 1.
[8] HuangS-F, ChenY-T, LeeW-C, ChangI-C, ChiuY-T, ChangY, et al., Identification of transforming hepatitis B virus S gene nonsense mutations derived from freely replicative viruses in hepatocellular carcinoma, PLoS One 9 (2014), e89753, https://doi.org/10.1371/JOURNAL.PONE.0089753.
[9] U.L. ASK, W.H.C. MM, R.K. PHH, The preS2/S region of integrated hepatitis B virus DNA encodes a transcriptional transactivator, Nature 343 (1990) 457–461, https://doi.org/10.1038/343457A0.
[10] S.F.H. SSJ, Y.T.C. MSH, I.C.C. HJJ, et al., Dysregulation of the TGFBI gene is involved in the oncogenic activity of the nonsense mutation of hepatitis B virus surface gene sW182, Biochim. Biophys. Acta 1842 (2014) 1080–1087, https://doi.org/10.1016/J.BBADIS.2014.03.007.
[11] P.Y.H. WSS, Human carbonic anhydrases and carbonic anhydrase deficiencies, Annu. Rev. Biochem. 64 (1995) 375–401, https://doi.org/10.1146/ANNUREV.BI.64.070195.002111.
[12] Hewett-EmmettD, Evolution and distribution of the carbonic anhydrase gene families, EXS (2000) 29–76, https://doi.org/10.1007/978-3-0348-8446-4_3.
[13] TheparambilSM. DeitmerJW, BeckerHM. RuminotI, The role of membrane acid/base transporters and carbonic anhydrases for cellular pH and metabolic processes, Front. Neurosci. 8 (2014), https://doi.org/10.3389/FNINS.2014.00430.
[14] MahonBP. MbogeMY, FrostSC. McKennaR, Carbonic anhydrases: role in pH control and cancer, Metabolites 8 (2018), https://doi.org/10.3390/METABO8010019.
[15] C.C.H. HYD, M.D.Y. SCL, A.L.C. GML, et al., Carbonic anhydrase III promotes transformation and invasion capability in hepatoma cells through FAK signaling pathway, Mol. Carcinog. 47 (2008) 956–963, https://doi.org/10.1002/MC.20448.
[16] A.T. OK, V.H. DC, M.M. CC, et al., pH regulators to target the tumor immune microenvironment in human hepatocellular carcinoma, OncoImmunology 7 (2018), https://doi.org/10.1080/2162402X.2018.1445452.
[17] Y.M.J. WJH, I.U.F. HSL, P.L.L. FYS, et al., Expression of hypoxic marker carbonic anhydrase IX predicts poor prognosis in resectable hepatocellular carcinoma, PLoS One 10 (2015), https://doi.org/10.1371/JOURNAL.PONE.0119181.
[18] PS, RDV-J, ALH, Regulation of tumor pH and the role of carbonic anhydrase 9, Cancer Metastasis Rev. 26 (2007) 299–310, https://doi.org/10.1007/S10555-007-9064-0.
[19] V.A. CTS, K.D.A. ADF, S.M.M. FC, et al., Inhibition of carbonic anhydrase IX targets primary tumors, metastases, and cancer stem cells: three for the price of one, Med. Res. Rev. 38 (2018) 1799–1836, https://doi.org/10.1002/MED.21497.
[20] J.H.Y. SJY, S.J.M. JHL, M.S.K. ESJ, et al., Inhibition of hypoxia-inducible carbonic anhydrase-IX enhances hexokinase II inhibitor-induced hepatocellular carcinoma cell apoptosis, Acta Pharmacol. Sin. 32 (2011) 912–920, https://doi.org/10.1038/APS.2011.24.
[21] KopacekJ. PastorekovaS, PastorekJ, Carbonic anhydrase inhibitors and the management of cancer, Curr. Top. Med. Chem. 7 (2007) 865–878, https://doi.org/10.2174/156802607780636708.
[22] J.H.T. FHS, C.V.R. SJL, B.Z. XD, et al., Carbonic anhydrase-related protein CA10 is an evolutionarily conserved pan-neurexin ligand, Proc. Natl. Acad. Sci. U. S. A 114 (2017) E1253–E1262, https://doi.org/10.1073/PNAS.1621321114.
[23] K.F.-A.I.N. NO, S.O. KT, cDNA sequence of human carbonic anhydrase-related protein, CA-RP X: mRNA expressions of CA-RP X and XI in human brain, Biochim. Biophys. Acta 1518 (2001) 311–316, https://doi.org/10.1016/S0167-4781(01)00193-2.
[24] I.N. EM, T.T. KT, S.O. YO, Overexpression of carbonic anhydrase-related protein VIII in human colorectal cancer, J. Pathol. 201 (2003) 37–45, https://doi.org/10.1002/PATH.1404.
[25] T.T. TI, Y.A. IN, J.F. TM, et al., Carbonic anhydrase-related protein VIII increases invasiveness of non-small cell lung adenocarcinoma, Virchows Arch. : an int. j. pathol. 448 (2006) 830–837, https://doi.org/10.1007/S00428-006-0199-0.
[26] I.N. KM, T.K. TT, T.T. NO, et al., Overexpression of carbonic anhydrase-related protein XI promotes proliferation and invasion of gastrointestinal stromal tumors, Virchows Arch. : an int. j. pathol. 447 (2005) 66–73, https://doi.org/10.1007/S00428-005-1225-3.
[27] FabregatI. Dysregulation, Of apoptosis in hepatocellular carcinoma cells, World J. Gastroenterol. : WJG 15 (2009) 513, https://doi.org/10.3748/WJG.15.513.
[28] JMS, MS, PRG, Cell death and hepatocarcinogenesis: dysregulation of apoptosis signaling pathways, J. Gastroenterol. Hepatol. 26 (Suppl 1) (2011) 213–219, https://doi.org/10.1111/J.1440-1746.2010.06582.X.

[29] D.L. WS, D.C. SS, S.R.-R. KS, et al., Mcl-1 overexpression in hepatocellular carcinoma: a potential target for antisense therapy, J. hepatol. 44 (2006) 151–157, https://doi.org/10.1016/J.JHEP.2005.09.010.
[30] D.L. EJG, C.C. GC, Hepatocellular carcinoma and markers of apoptosis (bcl-2, bax, bcl-x): prognostic significance, Appl. Immunohistochem. Mol. Morphol. : Appl. Immunohistochem. Mol. Morphol. AIMM 10 (2002) 210–217, https://doi.org/10.1097/00129039-200209000-00004.
[31] BS, BE, KW, BHJ, SL, Two point mutations convert a catalytically inactive carbonic anhydrase-related protein (CARP) to an active enzyme, FEBS Lett. 398 (1996) 322–325, https://doi.org/10.1016/S0014-5793(96)01263-X.
[32] PatiarS. SwietachP, HarrisAL. SupuranCT, Vaughan-JonesRD, The role of carbonic anhydrase 9 in regulating extracellular and intracellular pH in three-dimensional tumor cell growths, J. Biol. Chem. 284 (2009), 20299, https://doi.org/10.1074/JBC.M109.006478.
[33] JH, HA, KH, KM, Carbonic anhydrase-related protein is a novel binding protein for inositol 1,4,5-trisphosphate receptor type 1, Biochem. J. 372 (2003) 435–441, https://doi.org/10.1042/BJ20030110.
[34] M.N. EP, T.S. PLC, S.L. RM, et al., The carbonic anhydrase domain of receptor tyrosine phosphatase beta is a functional ligand for the axonal cell recognition molecule contactin, Cell 82 (1995) 251–260, https://doi.org/10.1016/0092-8674(95)90312-7.
[35] Ali-EldinZA. MohamedAA, El-SerafyM. ElbedewyTA, Ali-EldinFA, AbdelAzizH, MicroRNAs and clinical implications in hepatocellular carcinoma, World J. Hepatol. 9 (2017) 1001, https://doi.org/10.4254/WJH.V9.I23.1001.
[36] F.D. GW, S.S. ZX, D.C. XH, et al., MicroRNA profile in HBV-induced infection and hepatocellular carcinoma, BMC Cancer 17 (2017), https://doi.org/10.1186/S12885-017-3816-1.
[37] D.O. RM, C.O. MO, MicroRNA-27b suppresses tumor progression by regulating ARFGEF1 and focal adhesion signaling, Cancer Sci. 107 (2016) 28–35, https://doi.org/10.1111/CAS.12834.
[38] MiyazakiH. TakahashiR, YamamotoY. TakeshitaF, OnoM. MinouraK, et al., Loss of microRNA-27b contributes to breast cancer stem cell generation by activating ENPP1, Nat. Commun. 6 (1) (2015), https://doi.org/10.1038/ncomms8318, 2015; 6: 1–15.
[39] Y.L. HZ, Z.H.K.X. LX, Overexpression of MicroRNA-27b inhibits proliferation, migration, and invasion via suppression of MET expression, Oncol. res. 25 (2017) 147–154, https://doi.org/10.3727/096504016X14732772150505.
[40] HL, JA-J, ZJ-Z, HJ-B, ZL, YY-X, Clinicopathological significance of miR-27b targeting Golgi protein 73 in patients with hepatocellular carcinoma, Anti Cancer Drugs 30 (2019) 186–194, https://doi.org/10.1097/CAD.0000000000000711.
[41] WuX. YeJ, WuP. WuD, ZhangZ. NiC, et al., miRNA-27b targets vascular endothelial growth factor C to inhibit tumor progression and angiogenesis in colorectal cancer, PLoS One 8 (2013), https://doi.org/10.1371/JOURNAL.PONE.0060687.
[42] ZhangC, ZouY, DaiDQ, Downregulation of microRNA-27b-3p via aberrant DNA methylation contributes to malignant behavior of gastric cancer cells by targeting GSPT1, Biomed. pharmacother. Biomed. pharmacoth. 119 (2019), https://doi.org/10.1016/J.BIOPHA.2019.109417.
[43] YamadaT. SuzukiM, SakuraiT. Kihara-NegishiF, HaraE, TenenDG, et al., Site-specific DNA methylation by a complex of PU.1 and Dnmt3a/b, Oncogene 25 (2006) 2477–2488, https://doi.org/10.1038/SJ.ONC.1209272.
[44] TachibanaM, MatsumuraY, FukudaM, KimuraH, ShinkaiY, G9a/GLP complexes independently mediate H3K9 and DNA methylation to silence transcription, EMBO J. 27 (2008) 2681–2690, https://doi.org/10.1038/EMBOJ.2008.192.